

Effects of electromigration on resistance changes in eutectic SnBi solder joints

Jia Sun · Guangchen Xu · Fu Guo ·
Zhidong Xia · Yongping Lei · Yaowu Shi ·
Xiaoyan Li · Xitao Wang

Received: 28 October 2010 / Accepted: 6 January 2011 / Published online: 19 January 2011
© Springer Science+Business Media, LLC 2011

Abstract The motivation of this study is tried to explore the relationship between resistance changes and microstructure evolution of eutectic SnBi solder joints under 10^4 A/cm^2 of current density and 50 °C of ambient temperature. A novel type of one-dimensional solder joints was employed to achieve a true uniform distribution of current density, and a real-time data acquisition system was employed to investigate the voltage changes of the eutectic SnBi solder joints during electromigration process. This study suggested that the resistance remained initially due to the interaction between coarsened phase and Joule heating effect, and then increased due to the formation of continuous Bi-rich phase at anode interface, finally remained again due to the phase segregation of Bi- and Sn-rich phases.

Introduction

Massive movement resulting from high current density in solder joints is known as electromigration (EM). The failure in solder joints induced by EM is becoming a crucial reliability issue with continuously shrinking size of solder joints [1–3]. During the EM process, the metal atoms/ions accumulated at the anode interface can cause

the formation of hillock, while the depletion of metal atoms/ions at the cathode interface can cause the formation of valley [4]. In addition, when the two-phase eutectic materials are used as the interconnection material, the different α -rich and β -rich phases were usually found to segregate in the bulk region [3, 5, 6]. Since the electrical resistivity of pure metal is different from that of alloy, the resistance should be altered in solder joints when the phase segregation occurred under the continuous current stressing. Due to the physical law of resistance, when the cross-section area d and the length of solder joints both keep constant, the microstructure evolution will be the only one parameter to determine the resistance changes. Accordingly, resistance changes can be employed to investigate the different ongoing process of EM.

Currently, Pb-Sn is replaced by Pb-free solder alloy which has been an inevitable tendency. Pb-free solder systems bring in lots of additional complications, which may participate actively in the EM process [7]. Therefore, it is important to investigate how individual specimen behave during the EM process in Pb-free solder joints. Eutectic SnBi solder alloy has been considered as one of significant low melting point solder alloys in the recent years, which is one of the widely used binary solder alloys. What's more, similar to EM behaviors of SnPb solder alloy, phase segregation and redistribution can occur in SnBi solder alloy during the EM process as well [8].

Several researchers, i.e., Anderson reported that the resistivity changes of Sn3.0Ag0.5Cu solder joints were influenced complicatedly by the stress relief, solute redistribution, grain growth, and secondary phases at 423 K of isothermal aging [9]. Furthermore, in our previous EM study, the voltage changes of solder joints were believed to be affected mainly by Joule heating and accumulation of Bi-rich phase at the anode interface under the 10 A of the

J. Sun · G. Xu · F. Guo (✉) · Z. Xia · Y. Lei · Y. Shi · X. Li
College of Materials Science and Engineering, Beijing
University of Technology, Beijing 100124,
People's Republic of China
e-mail: guofu@bjut.edu.cn

X. Wang
State Key Laboratory for Advanced Metals and Materials,
University of Science and Technology, Beijing 100083,
People's Republic of China

current stressing and 80 °C of ambient temperature [10]. Resistance changes accompanying with microstructure evolution are hence considered to suffer the complex effects during the EM process. Moreover, a moderate ambient temperature and an appropriate current input need to be applied to solder joints to avoid the over-Joule heating effect. Hence, two things should be carefully reconsidered. First, current input needs to be decreased. It is known that the Joule heating was produced by current input, which drives resistance increase. Hence, a lower current input need to be explored; Second, the ambient temperature during EM process. Since, bulk intermetallic compounds (IMCs) can be easily formed in solder matrix at high ambient temperature which can migrate under the influence of EM. However, the bulk IMCs were unexpected for the purpose of investigation of phase evolution during EM. Hence, a lower ambient temperature of 50 °C was applied to avoid the formation of the bulk IMCs in solder matrix.

Therefore, a novel type of solder joints and a moderate ambient temperature of 50 °C were employed to understand the fundamental interaction between microstructure evolution and resistance changes in eutectic SnBi alloy during EM process. In addition, a high-rate real-time data acquisition system (DAQ) was developed to monitor the voltage changes of solder joints during the current stressing.

Experimental procedure

Fabrication of one-dimensional solder joints

Eutectic SnBi solder ball was pressed into a disk with thickness of 70 µm, and then it was cut to a square shape (0.7 × 0.7 mm). Then the oxygen-free high-conductivity copper sheet with a thickness of 0.5 mm was cut into 20 × 2 mm strips. Before soldering the joint, these Cu substrate specimens were cleaned by ultrasonic cleaners and then dried. Both squared solder dish and Cu stripes were placed into aluminum die. Most detailed information about specimen preparation can be found in our latest publication [11]. The prototypes were soldered by a reflow oven and then were dipped with the cold water onto joint region. A fine eutectic microstructure of the solder alloy can be obtained consequently. Configuration of the as-reflowed eutectic SnBi solder joints can be seen in Fig. 1a.

The fabricated solder joints were cold mounted into the epoxy resin to fabricate the conventional metallurgical polishing process. The ultimate solder joints processed a cross section of isosceles right triangle, as shown in Fig. 1b. Consequently, the corresponding area that the electron passed through can be calculated by knowing the

hypotenuse through the optical microscope (OM). Microstructure of the as-reflowed eutectic SnBi solder joints can be seen in Fig. 1c. Therefore, a current density of 10⁻⁴ cm²/A can be achieved under a constant current stressing of 5 A.

Solder joints without free surface

In order to investigate the relationship between resistance changes and microstructure evolution, the joined region was covered with epoxy resin to remove the free surface. The advantage of such process can be found in our previous publication [10]. As shown in Fig. 2, most regions of the Cu substrate were not covered with the epoxy resin, thus most of Joule heating can be dissipated effectively from the solder region.

Real-time data acquisition of voltage changes

A virtual instrument of DAQ system [10] was employed to monitor the voltage changes of solder joints during EM process. In addition, a four-point method was used to measure the resistance of solder joints under high current density. The effects on the resistance changes were from three parts which included copper substrates, IMCs, and solder matrix. To calculate the resistance changes, each joint was modeled as a series resistor, which was formed by (copper → IMCs → matrix → IMCs → copper), where the IMCs represented interfacial layers of Cu₆Sn₅ IMCs and Cu₃Sn IMCs. The total resistance of the solder matrix (R_s), IMCs (R_{Cu_3Sn} and $R_{Cu_6Sn_5}$), and copper substrate (R_{Cu}) can be expressed as follow:

$$R_t = R_s + 2R_{IMCs} + 2R_{Cu} \\ = \rho_{sm} \frac{L_{sm}}{A} + 2\rho_{IMCs} \frac{L_{IMCs}}{A} + 2\rho_{Cu} \frac{L_{Cu}}{A} \quad (1)$$

where R_t is the total resistance between voltage leads (Ω), A is the cross-sectional area of solder joints (0.5 × 10⁻³ cm²), and L is the length of the resistor (µm). When the cross-section area (A) of the solder joints keeps constant, the resistance changes R_t are determined by resistivity (ρ) and length of the resistor (L).

Microstructural observation was performed using a scanning electron microscopy (SEM), and elemental analysis was carried out by energy-dispersive X-ray (EDX) analysis in the SEM.

Results and discussion

A preliminary investigation indicated that voltage changes kept stable under a 5 A of current stressing at 50 °C of ambient temperature during initial current stressing 50 h of

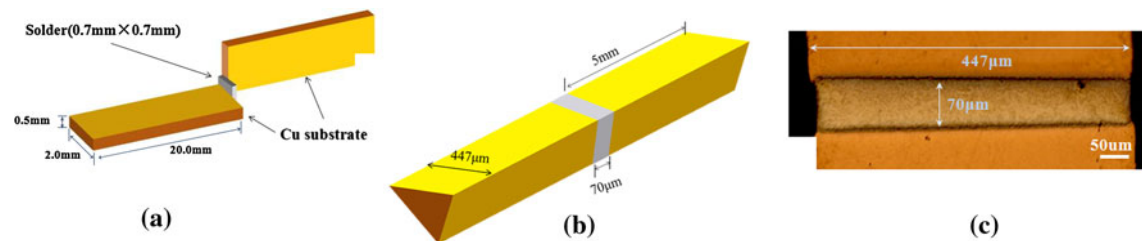


Fig. 1 Sample preparation of the eutectic SnBi solder joints: **a** schematic drawing of the as-reflowed solder joints; **b** three-dimensional of the as-fabricated cross section; **c** microstructure of the jointed region

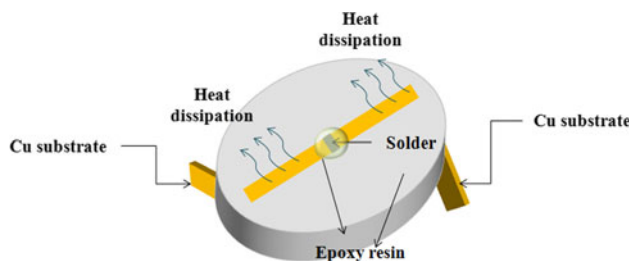


Fig. 2 Schematic drawing of the EM sample without free surface

EM process. Accordingly, a moderate current input can eliminate the effects of the Joule heating on the voltage changes.

Figure 3a shows the curve of voltage changes during 648 h of current stressing. The voltage remained the same within the initial 50 h of current stressing, which was defined as stage I, and then the voltage increased from 50 to 624 h, which was hence defined as stage II, and finally it remained at a high level of 46 mV, which was defined as stage III.

Figure 3b and c shows the microstructure of the solder joints after 48 and 600 h of current stressing, respectively. Figure 4b reveals that the microstructure of the solder matrix is still the lamella morphology after 48 h of current stressing. Figure 4c reveals that the solder matrix has been divided into two phases in solder matrix. It indicates that,

from 48 to 600 h, Bi atoms/ions can migrate to the anode side under the driving force of electron wind flow, and then form a continuous pure Bi-rich phase. The Sn atoms/ions were crowded toward to the cathode side of solder joints, which in turn blocked the migration of small clod of Bi. Accordingly, a small amount of Bi-rich phase was still remained at the cathode and distributed along the diffusion channel in the continuous Sn-rich phase.

Figure 4a and b shows the microstructure of solder joints as reflow and after 48 h of current stressing, respectively. Two square areas of $20 \times 20 \mu\text{m}$ were intentionally selected from the period of the cathode side before and after current stressing, as shown in Fig. 3c and e. Using ImageJTM, a public-domain Java-based professional image processing software, quantification of the coarsened Bi-rich phase becomes possible. Before counting and measuring objects in the eutectic Sn–Bi microstructure, the particle analyzer should be configured. By setting a single size of $0.05 \mu\text{m}^2$, particles smaller than this value can be ignored. Accordingly, the profiles of the Bi-rich phase before and after EM were obtained by ImageJTM, as shown in Fig. 5d and f. Under such conditions, the area fraction of Bi-rich phase as reflow was decreased from 57.91 to 44.75%. It indicates that 13.16% of the Bi-rich phase in cathode side of solder joints had been migrated to the anode side under the influence of the current density calculated to be 57.91 and 44.75% for Bi-rich phase after 48 h

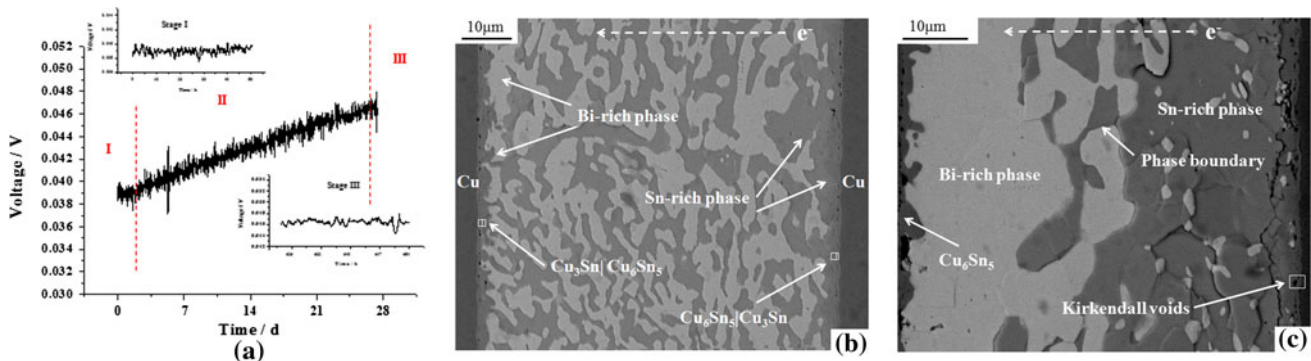


Fig. 3 The relationship between voltage changes and microstructure evolution of eutectic SnBi solder joints: **a** the voltage–time behavior under current density of 10^{-4} A/cm^2 stressing of 5 A at 50 °C; **b** the

microstructure after current stressing of 48 h; **c** the microstructure after current stressing of 600 h

current stressing. It indicates that 13.16% of the Bi-rich phase in cathode side of solder joints had been migrated to the anode side under the influence of the electron word force.

Figure 5a and b is the enlarged SEM images from Fig. 3c. As shown in Fig. 5, the migration of Bi atoms/

ions prompted continuous increase of Bi-rich layer at anode side, which induced segregation of Bi-rich phase with Sn-rich phase. The pure metal layer of Bi- and Sn-rich phases can be defined as two resistors of Sn and Bi, respectively. Consequently, the Eq. 1 can be expressed as follow:

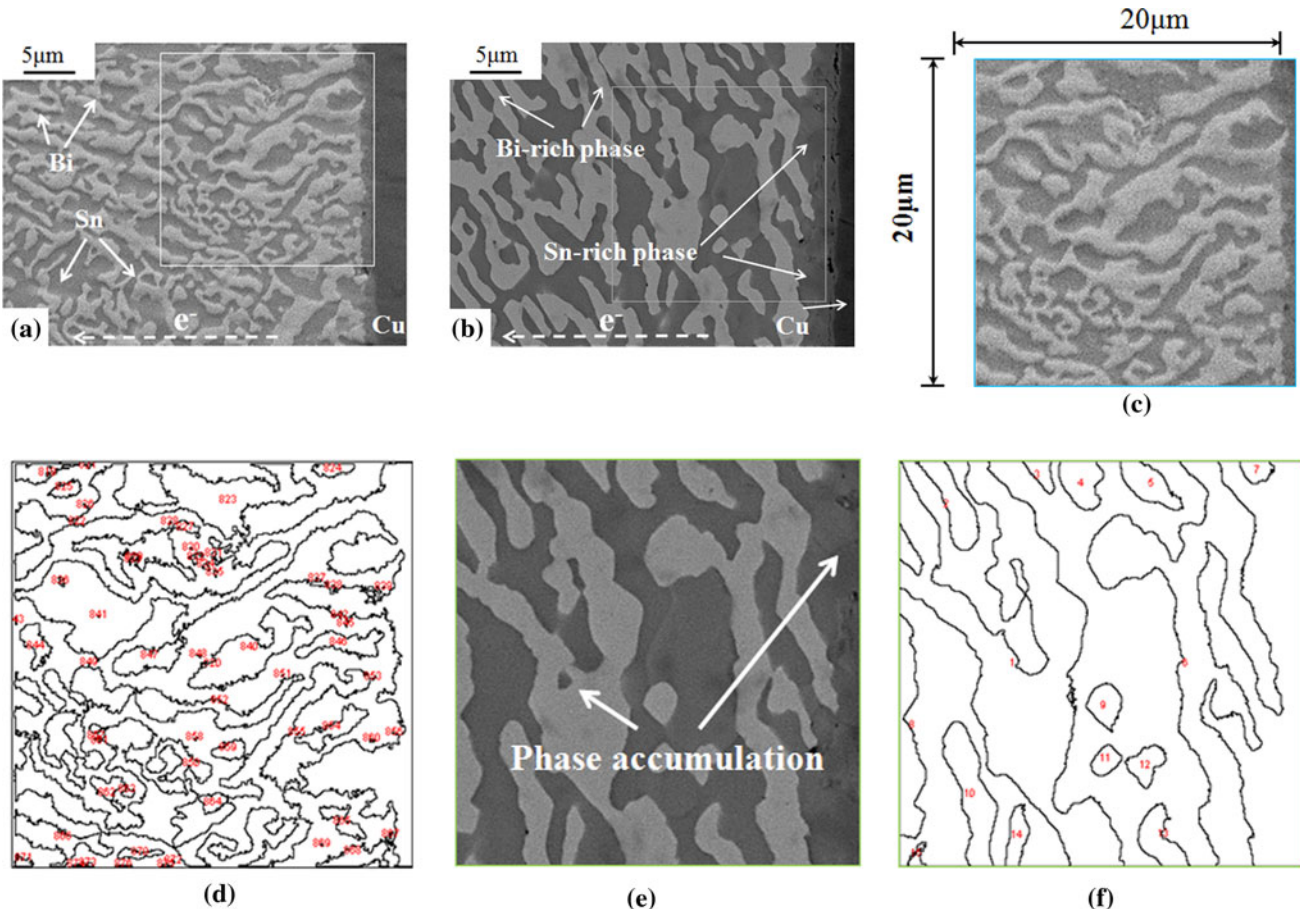
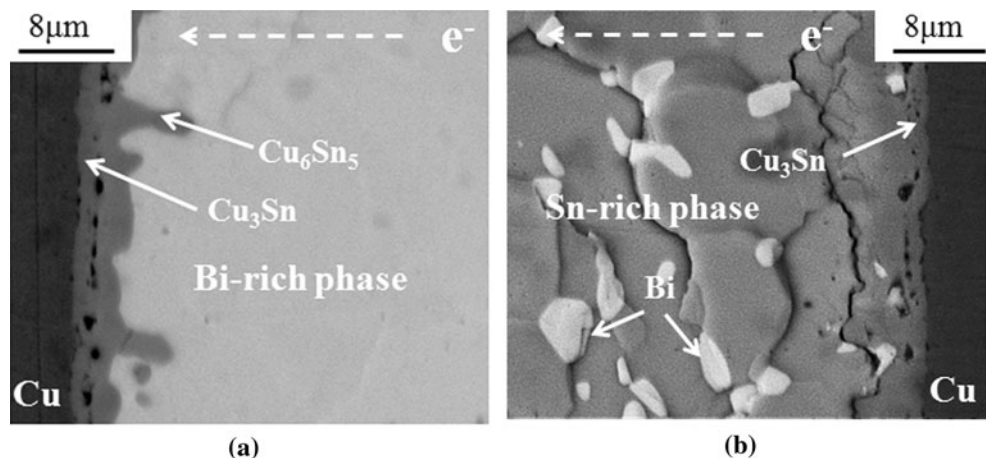


Fig. 4 Microstructural evolution of eutectic Sn–Bi solder during EM: **a** initial microstructure; **b** coarsened microstructure after 48 h of current stressing; **c** the profile of the Bi-rich phases in **(a)**; **d** the

profile of the Bi-rich phases obtained by ImageJTM; **e** the profile of the Bi-rich phase in **(b)**; **f** the profile of the Bi-rich phases obtained by ImageJTM

Fig. 5 Interfacial microstructure of solder joints after 600 h of current stressing: **a** the anode side; **b** the cathode side



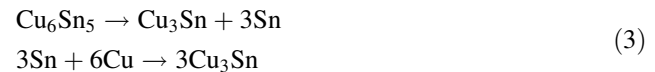
$$R_{t_2} = \frac{1}{A} (\rho_{\text{Sn}} L_{\text{Sn}} + \rho_{\text{Bi}} L_{\text{Bi}} + 2\rho_{\text{IMCs}} L_{\text{IMCs}} + 2\rho_{\text{Cu}} L_{\text{Cu}}) \quad (2)$$

where R_{t_2} is the total resistance of the solder joints after 600 h of current stressing. As shown in Table 1, the resistivity of Bi is much higher than that of eutectic SnBi solder alloy. Therefore, the sum of resistance of pure Sn and pure Bi is larger than that of the alloy solder matrix.

In our study, phase coarsening can induce decline of resistance, while the Joule heating can induce resistance increased. Thus, the resistance of the solder joints kept constant at stage I. At the stage II, a Bi-rich layer can be formed at the anode side after 120 h of current stressing at 25 °C. According to Eq. 1, the Bi-rich layer can be defined as an independent resistor with a higher resistivity which can further prompt the increase of the voltage. Hence the Bi-rich layer which formed in the interface of the solder joints induced the resistance of solder joints at stage II. Meanwhile, the thickness of the Bi-rich layer increased linearly with time until the different phase separated completely. Finally, as the phase separation finished completely after 600 h of current stressing, the resistance kept constant at the stage III.

Simultaneously, the scalloped-type Cu₆Sn₅ IMCs and layer-type Cu₃Sn IMCs were formed at the interface of the solder joints as illustrated in Fig. 5a and b. Besides, an

amount of Kirkendall voids was found at the interface between Cu₃Sn IMCs and Cu₆Sn₅ IMCs, which was caused by the diffusion of atoms/ions along with the direction of electron wind flow. Since Cu₆Sn₅ IMCs tend to convert to more stable status of Cu₃Sn IMCs and release the Sn atoms. The transformation between Cu₆Sn₅ IMCs and Cu₃Sn IMCs can be express as below



As shown in Eq. 3, the Cu₃Sn IMCs were formed by three Cu atoms and a Sn atom. Since, the ratio of Cu atoms and the Sn atom in Cu₆Sn₅ IMCs was not exactly accurate to 6:5, as listed in Table 2. Interstitial Cu atoms can be existed inside lattice of Cu₆Sn₅ IMCs. The Cu atoms which were used to form Cu₃Sn IMCs were from Cu₆Sn₅ IMCs and Cu substrate. As shown in Fig. 6a and b, the thickness increase of Cu₃Sn IMCs layer and formation of the voids can be explained as follow: At the anode side, as shown in Fig. 6a, the Cu₃Sn IMCs layer formed by a Sn atom (released from Cu₆Sn₅ IMCs) and three Cu atoms (came from Cu substrate), then the formation of continuous Cu₃Sn IMCs layer blocked the movement of Sn atoms which move from Cu₆Sn₅ IMCs to Cu substrate. With the effects of electric wind flow, Cu atoms from Cu₆Sn₅ IMCs migrated to the interface which was between Cu₆Sn₅ IMCs and Cu₃Sn IMCs, formed Cu₃Sn IMCs with the Sn atoms. The voids hence left because of the loss of Cu atoms.

At the cathode side, as shown in Fig. 6b, the Cu atoms from cooper substrate accumulated at the interface between Cu substrate and Cu₆Sn₅ IMCs with the effects of EM, and then formed the Cu₃Sn IMCs with Sn atoms which were released from Cu₆Sn₅ IMCs. The continuous Cu₃Sn IMCs layer blocked movement of Cu atoms which came from Cu substrate. Thus, the increase thickness of Cu₃Sn IMCs consumed the Cu atoms which migrated from Cu₆Sn₅ IMCs under the influence of EM, the voids hence left because of the loss of Cu atoms.

Voids formation induced by the growth of the IMCs layer can trigger the current crowding, which further induced void propagation and caused solder joints failure finally. Therefore, the resistance can change ultimately.

Table 1 Resistivity value of the employed metal/alloy

Metals/alloys	Electrical resistivity μ (Ω cm)
Sn	11.9
Cu	1.68
Bi	129
Eutectic SnBi	38.3

Table 2 EDX result of Cu₆Sn₅ IMCs

Element	Weight percentage (%)	Atom percentage (%)
Cu K	39.63	55.08
Sn L	60.37	44.92
Amounts	100.00	

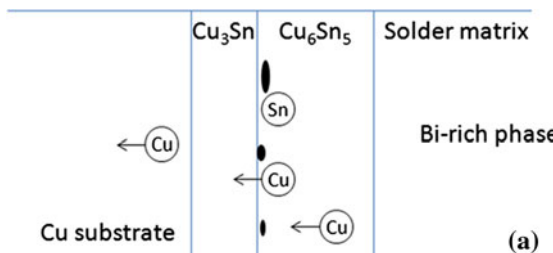
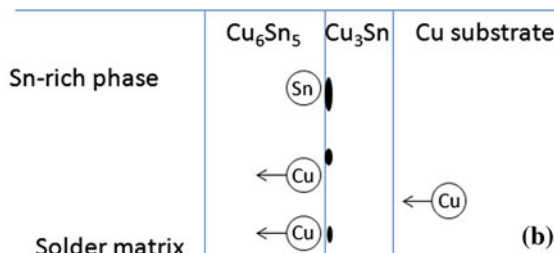


Fig. 6 Schematic drawing of formation of IMCs and voids: **a** the anode side; **b** the cathode side



Conclusions

1. A real-time DAQ based on the four-point method was developed to collect voltage changes during the EM process and assisted to explore the relationship between microstructure evolution and resistance changes in eutectic SnBi solder joints.
2. Under the current density of 10^4 A/cm 2 and the ambient temperature of 50 °C, the resistance kept 0.1925 Ω during the initial 24 h of stage I, which was caused by the balance between phase coarsen and Joule heating. At the stage II, the resistance increased from 192.5 to 230 mΩ during the 50 to 624 h, which was caused by the formation of Bi-rich phase at anode interface. Finally, the resistance kept 230 mΩ during the 624 to 648 h at the stage III, which was caused by phase segregation of Bi- and Sn-rich phases.

Acknowledgements The authors acknowledge the financial support of this study from the Beijing Natural Science Foundation Program and Scientific Research Key Program of the Beijing Municipal Commission of Education (KZ200910005004), the Academic

Innovation Group Supporting Program of Beijing Municipality, and the China Scholarship Council (2008654006). The authors also thank C. Henry Wang of Henkel Corp. for providing the eutectic Sn–Bi solder balls.

References

1. Guo F, Xu GC, He HW (2009) J Mater Sci 44:5595. doi: [10.1007/s10853-009-3787-y](https://doi.org/10.1007/s10853-009-3787-y)
2. Daghfal JP, Shang JK (2007) J Electron Mater 36:1372
3. He HW, Xu GC, Guo F (2010) J Mater Sci 45:929. doi: [10.1007/s10853-009-4022-6](https://doi.org/10.1007/s10853-009-4022-6)
4. He HW, Xu GC, Guo F (2010) J Mater Sci 45:334. doi: [10.1007/s10853-009-3939-0](https://doi.org/10.1007/s10853-009-3939-0)
5. Huynh QT, Liu CY, Chen C, Tu KN (2001) J Appl Phys 89:4332
6. Lee A, Ho CE, Subramanian KN (2007) J Mater Res 22:3265
7. Lu M, Shih DY, Lauro P, Goldsmith C, Henderson DW (2008) Appl Phys Lett 92:211909
8. Chen CM, Chen LT, Lin YS (2007) J Electron Mater 36:168
9. Cook BA, Anderson IE, Harringa JL (2003) J Electron Mater 32:1384
10. Guo F, Xu GC, Sun J (2009) J Electron Mater 38:2756
11. Zhang RH, Xu GC, Wang XT, Guo F, Lee A, Subramanian KN (2010) J Electron Mater 39:2513